Ultrasound in Med. & Biol., Vol. 33, No. 9, pp. 1368–1375, 2007

0301-5629/07/$–see front matter

ELSEVIER

doi:10.1016/j.ultrasmedbio.2007.03.012

● *Original Contribution*

NONINVASIVE ULTRASONIC MEASUREMENT OF REGIONAL AND LOCAL PULSE-WAVE VELOCITY IN MICE

Ross Williams,* Andrew Needles,* Emmanuel Cherin,* Yu-Qing Zhou,†
R. Mark Henkelman,† S. Lee Adamson,‡ and F. Stuart Foster*†

*Sunnybrook Health Sciences Centre, Toronto, ON, Canada; †Mouse Imaging Centre, Hospital for Sick Children, Toronto, ON, Canada; and ‡Samuel Lunenfeld Research Institute, Mount Sinai Hospital, Toronto, ON, Canada

(*Received* 26 *July* 2006; *revised* 7 *March* 2007; *in final form* 23 *March* 2007)

Abstract—Mouse models of human disease are increasingly used to study the nature of cardiovascular diseases such as atherosclerosis. The pulse wave velocity (PWV) provides an indirect measure of arterial stiffness and can be useful for characterizing disease progression. In this study, the PWV was measured noninvasively in the left common carotid artery of seven young mice using two image-guided approaches: a regional transit-time (TT) method and a local flow-area (QA) method. The QA approach measures the cross-sectional area and volume flow through the vessel using high frame-rate retrospective colour flow imaging. The QA method was found to correlate well with the TT method ($r^2 = 0.80, p < 0.001$). The mean difference between methods was 0.05 ± 0.21 m/s. This study demonstrates the feasibility of measuring both regional and local PWV in mice using image-based high-frequency ultrasound methodologies. (E-mail: williams@sri.utoronto.ca) **© 2007 World Federation for Ultrasound in Medicine & Biology.**

Key Words: **Pulse wave velocity, Local arterial stiffness, Colour flow imaging, Volume flow estimation, Mouse carotid artery.**

INTRODUCTION

Approximately one third of all deaths in Canada are caused by heart disease, diseases of the blood vessels and stroke (Statistics Canada 2003). Many forms of cardiovascular disease (CVD) are associated with arterial stiffening and stenosis (O'Rourke et al. 2002). In atherosclerosis, a major cause of arterial stiffening, the elasticity of the vessel wall is reduced due to the accumulation of fibrous plaques within the artery and the ageing of elastin. Animal models of human disease are increasingly employed to better understand the patho-physiological mechanisms of CVD. For example, arterial properties have been studied in transgenic mice designed to develop atherosclerosis (Hartley et al. 2000). To quantify risk factors associated with CVD, various interdependent indices of arterial fitness have been developed, including arterial distensibility, arterial compliance, elastic modulus and pulse wave velocity (PWV) (Nichols and O'Rourke 1990). To assist in the translation of small animal experimental studies to human clinical applications, measurement techniques are required that can accurately quantify arterial function in both humans and small animals.

The PWV is commonly employed to assess arterial stiffness. It is usually evaluated by measuring the difference in the arrival times of the initiation of the pressure wave at two locations a known distance apart, with stiffer vessels having higher PWV (O'Rourke et al. 2002). In humans, transit time (TT) methods of PWV estimation have been performed using manometry (Latham et al. 1985), arterial tonometry (Kelly et al. 1989) and with ultrasound measurements of wall motion (Benthin et al. 1991) and blood velocity (Lehmann et al. 1993). In small animals, Doppler ultrasound-based TT approaches have been applied to mice (Hartley et al. 1997) and rats (Mitchell et al. 1997). The TT methods provide an average PWV over the propagation pathway, which varies with vessel diameter, wall thickness and local elastic modulus (Li 2004). Consequently, regional measurements of PWV may mask short but significant variations in arterial properties. In early stage atherosclerosis, millimeter-size plaques are scattered along the vessel wall (Chubachi et al. 1994). To overcome limitations related to applying the TT method over short propagation

Address correspondence to: Ross Williams, Imaging Research, Sunnybrook Health Sciences Centre, S-639, 2075 Bayview Ave, Toronto, ON, Canada, M4N 3M5. E-mail: williams@sri.utoronto.ca

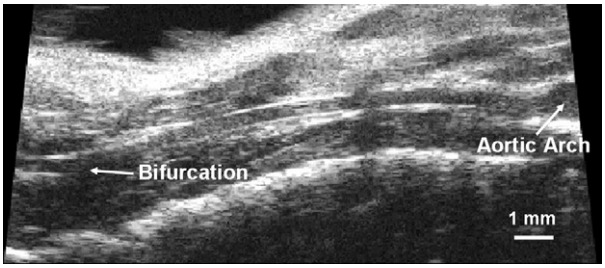

Fig. 1. The left common carotid artery in the mouse imaged at 40 MHz, from the aortic arch to the bifurcation. Transit-time measurements were performed at distal and proximal sites, located 1.5 mm upstream from the bifurcation and 1 mm downstream from the aortic arch, respectively. The local flow-area measurement was performed at the carotid midsection.

lengths, ultrasonic methods of measuring the local PWV have been proposed, including approaches based on assessing temporal and longitudinal gradients of vessel diameter (Brands et al. 1998), tissue Doppler imaging of wall motion (Eriksson et al. 2002), flow-area (QA) relations (Rabben et al. 2004) and laser vibrometry measurements of radiation force-induced pressure disturbances (Zhang and Greenleaf 2006).

In this study, we have compared a TT method of measuring the PWV with a QA method in the left common carotid artery (LCCA) of seven CD-1 mice (Fig. 1). The TT technique was used to measure a regional PWV over a segment of the carotid artery from the aortic arch to the bifurcation. The QA method was applied to determine the local PWV at the midsection of the carotid segment. The objectives of this study were to assess the feasibility and comparative accuracy of the QA method against the TT method and to demonstrate simple image-based methodologies for performing PWV measurements in mice.

MATERIALS AND METHODS

Transit-time method

The TT method estimates the PWV from the pressure wave transit time, Δt, between two measurement locations separated by a known distance, Δd:

$$\mathrm{PWV} = \frac{\Delta d}{\Delta t} \tag{1}$$

Hartley et al. (1997) demonstrated that the upstroke of the velocity waveform is coincident with the pressure upstroke in mice. Pulsed-wave Doppler ultrasound velocity measurements were consecutively performed at the distal and proximal locations while simultaneously recording the electrocardiogram (ECG) signal, over a short period of time during which the mouse was observed to have stable heart and breathing rates. The transit time was found by subtracting the distal arrival time between the ECG R-wave peak and the foot of the velocity upstroke from the similarly determined proximal arrival time. The foot is defined as the point at the end of diastole when the steep rise of the wavefront begins (Zhang and Greenleaf 2006). It is commonly used as a marker because the peak velocity and overall pulse shape may be altered by reflected waves (Li 2004). As a threshold for consistent detection of the upstroke, the arrival times were calculated relative to the time at which twenty percent of the peak value was attained.

The LCCA was chosen as a measurement target because it was easily accessible and offered a uniform and branch-free pathway over approximately 10 mm between the aortic arch and bifurcation. The distance between the measurement sites was determined from a B-mode image encompassing both the distal and proximal locations (Fig. 1). Proximal velocity measurements were taken 1 mm downstream from the aortic arch. Distal velocity measurements were taken 1.5 mm upstream from the bifurcation (Fig. 2).

TT measurements were performed using a VisualSonics Vevo770 ultrasound biomicroscope (VisualSonics Inc, Toronto, ON, Canada). The mechanically scanned single-element transducer had a 6 mm focal length and f-number of 2. B-mode data were acquired at 40 MHz, with a 30 frames-per-second (fps) frame rate. Doppler data were acquired at 30 MHz, with a 50 kHz pulse-repetition frequency (PRF). The ECG signal was detected using a heart rate monitoring system (VisualSonics Inc, Toronto, ON, Canada) smoothed with a 1 kHz low-pass filter and digitized by the Vevo770 system at 8 kHz. Results were processed using VisualSonics analysis software and Matlab (The Mathworks Inc, Natick, MA, USA).

Flow-area method

With the QA method, the PWV in an artery is estimated as the ratio between the change in flow and the change in cross-sectional area during the reflection-free period of the cardiac cycle. From the wave equation for arterial propagation and the characteristic impedance relation, it can be shown that (Rabben et al. 2004):

$$\mathrm{PWV} = \frac{\mathrm{d}Q}{\mathrm{d}A} \tag{2}$$

where Q is the volume flow through the vessel and A is the cross-sectional area of the vessel. In humans, the early systolic wave is reflection free (Li 2004). We have assumed the same to be true in the mouse.

In the QA method employed in this study, the area and flow were determined directly from high frame-rate colour flow data acquired in cross-section at the midpoint

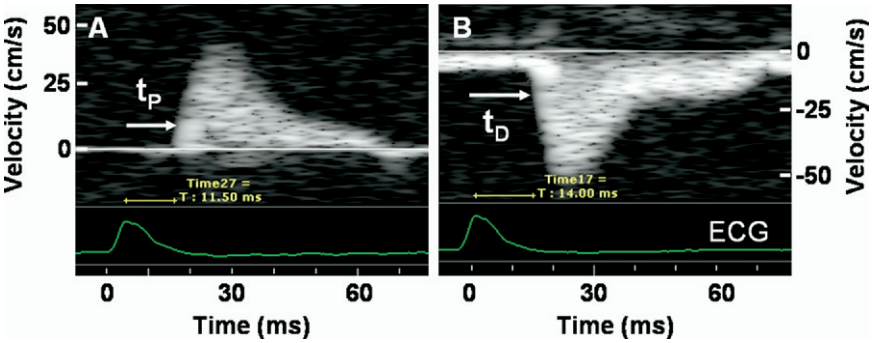

Fig. 2. (A) Typical pulsed-wave Doppler waveform measured at the proximal measurement location. The arrival time of the velocity upstroke relative to the ECG R-wave peak is denoted t_P. (B) Pulsed-wave Doppler waveform observed at the distal measurement location. The arrival time is denoted t_D. The waveforms in (A) and (B) are inverted because of differences in the flow direction relative to the transducer. The proximal and distal measurement sites were separated by 8.5 mm and the average PWV was found to be 3.3 m/s.

of the LCCA (Fig. 3). The carotid artery was segmented in each frame and a mask was generated to extract the colour flow data from within the vessel. The cross-sectional area was calculated over the region of flow in each frame of the colour flow data set, while the volume flow was calculated by averaging the velocities over the vessel in each frame and multiplying by the corresponding area. The PWV was determined from the slope of the resulting flow-area parametric relation over times corresponding to the reflection-free period of the cardiac cycle (Fig. 4). The area and flow were measured with 1 ms temporal resolution and a 400 Hz low-pass 9th-order Butterworth filter was used to smooth the signals.

High frame-rate B-mode and colour flow data sets were acquired using the ECG-gated, EKV™ retrospective imaging mode on the VisualSonics Vevo770 (Cherin et al. 2006). Using this technique, M-mode data collections were sequentially performed at a series of closely spaced locations across the imaging plane, with simultaneous recording of the ECG signal at each location. A postprocessing algorithm rearranged the ECG-gated M-mode acquisitions into a high-frame-rate series of B-mode images, with the resulting B-mode frame-rate dependent on the PRF used to collect the M-mode data. A single-element transducer with a focal length of 6 mm and f-number of 2 was used. Retrospective B-mode and colour flow data were simultaneously acquired at 40 MHz centre frequency with a 1000 fps effective frame rate. Conventional B-mode and pulsed-wave Doppler data were collected at 40 MHz, 30 fps and 30 MHz, 50 kHz PRF, respectively. Image data were processed off-line with Matlab.

For the colour flow data, the axial velocities were estimated using an autocorrelation algorithm (Jensen 1996) implemented by VisualSonics Inc, which was applied to the EKV M-mode data sets before their reorganization into a high-frame-rate series of B-mode images. The vessel was imaged at a slight angle relative to the true cross-section, to minimize skewing of the area while allowing for the detection of unidirectional flow. In cross-section, the Doppler correction angle could not be accurately determined, preventing assessment of the true blood velocity. To determine the true blood velocity, the vessel was imaged longitudinally a short time after the retrospective acquisition and the velocity in the centre of the vessel was measured with pulsed-wave Doppler, with an angle of approximately 60° between the ultrasound beam and the vessel. The retrospectively determined cross-sectional colour flow velocities were then scaled such that the velocity in the middle of

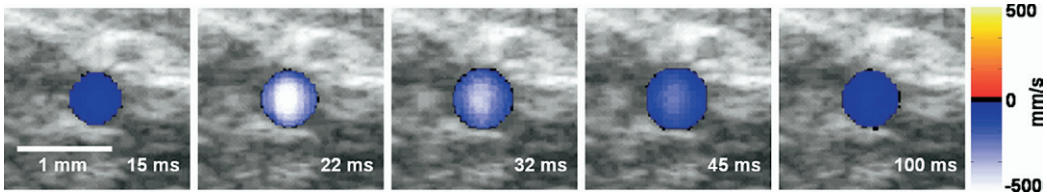

Fig. 3. Frames extracted from a retrospective movie of blood flow through a cross-section of the carotid artery. The imaging was performed at 40 MHz, with an effective frame rate of 1000 frames-per-second. The cardiac cycle had a duration of 138 ms.

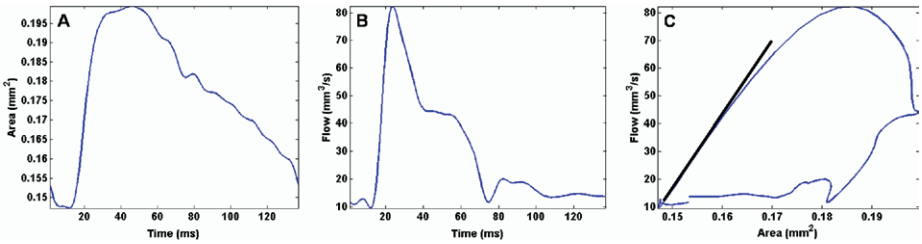

Fig. 4. PWV flow-area results. (A) Cross-sectional area of the carotid artery during one cardiac cycle. (B) Flow over one cardiac cycle through the carotid artery. (C) The PWV is equal to the slope of the flow-area relation during the reflection free, early systolic phase of the cardiac cycle.

the vessel agreed with the mean angle-corrected pulsed-wave Doppler velocity measurement performed longitudinally in the vessel's centre.

Experimental protocols

Animal experiments were performed under a protocol approved by the Animal Care Committee of Sunnybrook Health Sciences Centre. Seven healthy CD-1 female mice (CD-1 Swiss albino strain, Charles River Laboratories, St Constant, QC, Canada) were examined at 5 to 6 mo of age. The mice were anesthetized with isoflurane (2% oxygen) and positioned on a mouse imaging stage that provided heart rate monitoring. Depilatory cream (Nair™, Carter-Horner, Mississauga, ON, Canada) was used to remove fur from the throat and chest and ultrasound gel (Aquasonic 100, Parker Laboratories, Fairfield, NJ, USA) was used as a coupling medium between the transducer and the skin. Using B-mode imaging, the transducer was positioned to provide either a longitudinal section or cross section of the mouse carotid artery, with the region of interest located in the focal zone of the transducer.

RESULTS

Transit-time method

For the seven CD-1 mice, the average TT PWV in the LCCA was found to be 3.0 ± 0.4 m/s (mean ± SD). In each mouse, the measurements were repeated 10 times. The average propagation distance in each mouse, the proximal and distal pulse arrival times relative to the ECG R-wave peak and the corresponding PWVs are listed in Table 1. The heart rates were steady over the course of the experiment, ranging from 350 to 480 beats per minute (bpm). The propagation lengths measured in the LCCA ranged from 6.5 to 9.1 mm, with an average of 8.1 ± 0.9 mm. The average proximal and distal pulse arrival times were 15.1 ± 2.5 ms and 17.8 ± 2.6 ms, respectively. The average difference between the distal and proximal arrival times (*i.e.*, the transit time) was 2.7 ± 0.6 ms.

Thirty repeated measurements in the same mouse showed that the distal arrival time, measured from the peak of the ECG R-wave to the foot of the Doppler upstroke (at 20% of the peak amplitude), was 19.6 ± 0.4 ms and the proximal arrival time was 16.8 ± 0.4 ms. Repeated measurements of the distal-to-proximal length in the same mouse produced an average value of 8.3 ± 0.1 mm. The derived uncertainty on the PWV was found to be ±0.6 m/s.

Flow-area method

For the seven CD-1 mice, the average QA PWV at the midsection of the LCCA was found to be 2.97 ± 0.48 m/s. The measured values for each mouse are listed in Table 2.

The average cross-sectional area was found to be 0.16 ± 0.3 mm^2. The change in area was significant, ranging from 0.03 to 0.07 mm^2, with an average of 0.05 ± 0.01 mm^2. The average peak velocity was 374 ± 41 mm/s, while the mean velocity over the cardiac cycle was 126 ± 17 mm/s. The peak volume flow had a large range of values, from 45 to 95 mm^3/s, with an average of 63 ± 19 mm^3/s, while the average flow over the cardiac cycle was 21 ± 5 mm^3/s.

Method comparison

Correlation and bias plots showing how the QA PWV measurement method compared with the TT

Table 1. Transit-time measurements in the mouse common carotid artery

Mouse	Heart rate (bpm)	Propagation length (mm)	Proximal arrival time (ms)	Distal arrival time (ms)	PWV (m/s)
1	460	7.5	17.9	20.0	3.6
2	350	9.1	17.5	21.3	2.4
3	350	6.4	13.3	15.4	3.0
4	320	8.5	11.7	14.3	3.3
5	420	8.3	12.9	16.2	2.5
6	450	8.3	16.8	19.6	3.0
7	480	8.4	15.6	18.1	3.4

Table 2. Flow-area measurements in the mouse common carotid artery

Mouse	Average area (mm^2)	Change in area (mm^2)	Peak velocity (mm/s)	Average velocity (mm/s)	Peak flow (mm^3/s)	Average flow (mm^3/s)	PWV (m/s)
1	0.21	0.07	400	112	95	27	3.3
2	0.15	0.06	380	128	64	21	2.1
3	0.13	0.04	312	107	45	15	3.0
4	0.15	0.05	383	133	55	21	3.1
5	0.18	0.05	440	156	82	28	2.6
6	0.14	0.04	361	134	46	19	3.1
7	0.15	0.03	341	113	57	18	3.6

method are shown in Fig. 5. The upper and lower limits of agreement (bias ±2SD) represent the bounds within which 95% of the data can be expected to be found. The QA method was found to correlate well with the TT method ($r^2 = 0.80$, $p < 0.001$), with a mean difference between methods of -0.05 ± 0.21 m/s. The limits of agreement were $\pm 0.44 \pm 0.14$ m/s around the mean difference. The large errors on the upper and lower limits of agreement resulted from the limited sample size.

DISCUSSION

Transit-time method

The average PWV lies within the range of values previously reported for mice (Hartley et al. 1997). Vasodilation agents such as isoflurane tend to reduce arterial stiffness and lower the PWV from normal levels. In humans, which do not require anesthesia, a resting carotid PWV of 6 to 8 m/s has been reported (Nichols and O'Rourke 1990).

The low frequency nature of the pressure disturbance generated by cardiac contractions complicates accurate assessment of small time delays (Zhang and Greenleaf 2006). In theory, the measured apparent phase velocity should approximate the true phase velocity if the waveform is unaffected by reflected waves (Li 2004). The foot of the velocity upstroke, which has been shown to provide an accurate approximation to the true phase velocity (Greenwald et al. 1978), was found to be easily identifiable, although the shape of the pulse varied at the distal and proximal locations due to reflected waves and transducer orientation (Fig. 2). The arrival time was measured from the peak of the ECG R-wave to the time at which the upstroke attained 20% of its maximum value. Mitchell et al. (1997) compared various methods of automatically detecting the upstroke time and found that taking the maximum of the first-derivative of the signal was most effective.

The pre-ejection times, from the onset of electrical ventricular stimulation to the aortic opening, ranged from 13 to 18 ms. The pre-ejection times are relatively small compared with the average value of 23 ms measured by Hartley et al. (1997) in the mouse aortic arch, however, neither the mice nor the anesthetic used by Hartley were identical with those used in this study. Although there was a large variation between mice in the proximal and distal arrival times relative to the ECG R-wave, the relative proximal-distal transit times were much less variable, indicating that the variability had more to do

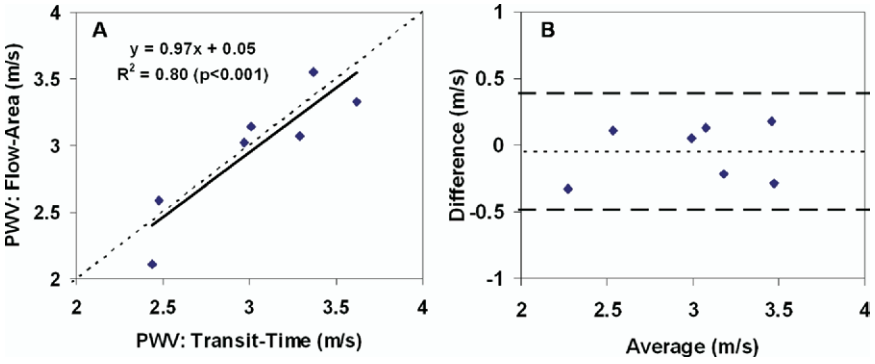

Fig. 5. The flow-area method compared with the transit-time method in the mouse LCCA. (A) Correlation plot. The dashed line represents the identity relation. (B) A Bland-Altman plot of the difference between the flow-area and transit-time methods, against the average of the two. The upper and lower limits of agreement (horizontal dashed lines) are ±2SD from the mean.

with the mouse physiology at the time of the measurement than with measurement uncertainty. Also, any constant display lag introduced by the VisualSonics system between the ECG signal and the Doppler signal would not affect relative transit-time measurements.

It was found that this technique was relatively insensitive to artifacts caused by the Doppler angle, since the angle did not significantly affect the relative time of the upstroke. It can be difficult to estimate the propagation distance if the vessel is tortuous or if the estimation length exceeds the field-of-view, neither of which was found to be a problem using an image-guided approach in the LCCA. Without image-guidance, the estimation length must be measured externally and is prone to error depending on the internal vessel geometry (Hartley et al. 1997).

The TT method is limited by the temporal resolution of the Doppler acquisition. Fast Fourier transform (FFT)-based Doppler-signal processors limit temporal resolution because finite sample lengths are required. Resolution is also limited by the FFT sampling rate, the ensemble overlap and the display resolution. For example, with a 50 kHz PRF, the sampling period is 20 μs, however, ensemble size and overlap limit the temporal resolution to approximately 250 μs on the VisualSonics system. Improved temporal resolution could potentially be achieved using a zero-crossing interval histogram processor (Hartley et al. 1997), which offers good sensitivity to rapid Doppler shifts.

Simultaneous assessment of the proximal and distal arrival times would also reduce variability compared with measurements performed consecutively, since the measurements would require less time and would therefore reduce the chance of temporal variations in the position or physiological state of the mouse.

Flow-area method

The average QA PWV is in agreement with the average TT PWV determined over a uniform 10 mm segment of the LCCA. As the mice used in this study were young and free of vascular lesions, local and regional measurements are likely to agree over uniform arterial segments. The coefficient of variation (SD/mean) was also similar between the TT and QA methods.

The changes in the cross-sectional area between diastole and systole correspond with the changes in diameter reported by Hartley et al. (2004). The volume flows were found to vary significantly between mice, however, a small change in area and velocity will cause a large variation in the flow through the vessel. Volume flows in the mouse carotid artery have not been previously reported.

The main sources of error in the QA method relate to flow estimation and area determination. The velocity correction angle could not be accurately determined when imaging the vessel in cross-section, so the retrospectively determined velocity over the centre of the vessel was scaled to agree with the mean velocity observed at the same location from a longitudinal perspective using pulsed-wave Doppler, in which the correction angle could be determined. The error involved in pulsed-wave Doppler measurements has been estimated by Rabben et al. (2004) to be approximately 15% when the true angle is 60° and the correction angle is 55°. The determination of the vessel area, which also influences the flow, was affected by the insonation angle and the segmentation method. A 15° angle relative to the true cross-section of a circular vessel results in a 4% area overestimation.

Assuming the heart rate of the mouse remains stable over the retrospective acquisition period, which requires approximately 2 min, the area and flow curves should be well aligned in time. However, variations in the arrival of the upstroke at each lateral location across the vessel relative to the ECG signal will affect the cross-sectional area and velocity measurements made from the high-frame-rate EKV movie. During the onset of the upstroke, when the area and flow are linearly related, these variations should average to approximate the true value.

The fast transit time of the pressure pulse across the cross-sectional imaging plane necessitates imaging with very high frame rates. Real-time acquisitions of the vessel in cross section would be superior to retrospective techniques, however, frame-rates are currently limited with the mechanical sector scanner. Expansion of the vessel wall caused by the pulse-wave pressure disturbance spans only 10 ms, meaning an effective frame rate of at least 200 fps is required. It is possible that such frame rates could be achieved in real time using high-frequency linear arrays like those now under development (Lukacs et al. 2006).

Reflected waves could influence the cross-sectional area and volume flow through the vessel. Assuming the QA method is applied sufficiently upstream from changes in arterial impedance, the influence of reflections on the area-flow slope should be minimized. The slope will be most accurate during the time immediately following the velocity upstroke, before reflected waves have had time to return. Over 6 mm, the return time of reflected waves is only 4 ms. The entire expansion of the vessel and velocity upstroke due to the passing pressure wave requires approximately 10 ms (Fig. 4).

Automated clutter-filter segmentation of the vessel was not feasible, because the clutter filter introduced artifacts when the wall velocity exceeded the cutoff velocity. Using a higher cutoff velocity caused slow flow around the edges of the vessel to be excluded. As a result, the vessel diameter was manually segmented in each frame of the colour flow data and a circular mask was

generated and applied to separate the blood flow from the surrounding vessel wall signal. Automated segmentation of the vessel would be required for efficient determination of PWV using the QA method. Pulse inversion techniques in combination with microbubble contrast agents could provide a improved means of automatically segmenting the flow within the vessel by suppressing linear echoes from the vessel wall while preserving nonlinear echoes from the agent (Hope Simpson et al. 1999).

The flow-area acquisition method may also be useful for measuring arterial distensibility, which is related to PWV by (Brands et al. 1998):

$$\mathrm{PWV} = \frac{1}{\sqrt{\rho \cdot D}} \tag{3}$$

with blood density ρ and distensibility D:

$$D = \frac{\Delta A/A}{\Delta P} \tag{4}$$

where ΔA is the change in cross-sectional area between diastole and systole, A is the local diastolic cross-sectional area and ΔP is the local pulse pressure. The brachial pulse pressure is often used in place of the local pulse pressure, however, due to wave propagation and reflections, differences may exist between the local and brachial pressures (Nichols and O'Rourke 1990). Nonetheless, $\Delta A/A$ is already measured directly with the flow-area method and it has previously been shown that local changes in diametric vessel excursions are indicative of arterial compliance (Hartley et al. 2004). Local distensibility measurements could potentially be of greater utility than PWV measurements, since the measurements are less prone to error and would likely be more clinically robust. Lower temporal resolution than that required for PWV estimation may also be possible, since the maxima and minima of the area curves are of interest and not the precise interrelation between the area and flow during systole.

CONCLUSIONS

This study demonstrated two image-guided approaches for estimating PWV in mice using high frequency ultrasound. A regional TT measurement was compared to a local QA measurement in the LCCA of seven young CD-1 mice. The QA method utilizes a high frame-rate retrospective colour flow imaging technique, with the PWV found from the slope of the flow-area relation during the reflection free period of the cardiac cycle. The PWV determined using the TT method over a segment of the carotid artery was found to correlate well with the local QA PWV observed at the LCCA midsection. While the regional PWV is useful for assessing systemic changes in vascular stiffness, such as those that occur naturally with ageing (Sutton-Tyrrell et al. 2001), the local PWV could assist in the early detection of subtle vascular abnormalities like those caused by atherosclerosis. A combination of these two ultrasonic techniques would permit a more comprehensive evaluation of arterial properties in mice.

Acknowledgments—This work was funded by the Canadian Institutes for Health Research, the National Cancer Institute of Canada/Terry Fox Foundation, the Ontario Research and Development Challenge Fund and VisualSonics Inc. The authors thank Allison Brown for her assistance with experimental animal protocols. FSF acknowledges a financial interest in VisualSonics Inc.

REFERENCES

Benthin M, Dahl P, Ruzicka R, Lindstrom K. Calculation of pulse-wave velocity using cross correlation effects of reflexes in the arterial tree. Ultrasound Med Biol 1991;17:461–469.

Brands PJ, Willigers JM, Ledoux LAF, Reneman RS, Hoeks APG. A noninvasive method to estimate the pulse wave velocity in arteries locally by means of ultrasound. Ultrasound Med Biol 1998;24: 1325–1335.

Cherin E, Williams R, Needles A, Liu G, White C, Brown AS, Zhou Y-Q, Foster FS. Ultrahigh frame rate retrospective ultrasound microimaging and blood flow visualization in mice *in vivo*. Ultrasound Med Biol 2006;32:683–691.

Chubachi N, Kanai H, Murata R, Koiwa Y. Measurement of local pulse wave velocity in arteriosclerosis by ultrasonic Doppler measurement. Proc IEEE Ultrason Symp 1994;1:1747–1750.

Eriksson A, Greiff E, Loupas T, Persson M, Pesque P. Arterial pulse wave velocity with tissue Doppler imaging. Ultrasound Med Biol 2002;28:571–580.

Greenwald SE, Newman DL, Bowden NLR. Comparison between theoretical and directly measured pulse propagation velocities in the aorta of the anaesthetized dog. Cardiovasc Res 1978;12:407–414.

Hartley CJ, Taffet GE, Michael LH, Pham TT, Entman ML. Noninvasive determination of pulse-wave velocity in mice. Am J Physiol Heart Circ Physiol 1997;273:H494–H500.

Hartley CJ, Reddy AK, Madala S, Martin-McNulty B, Vergona R, Sullivan ME, Halks-Miller M, Taffet GE, Michael LH, Entman ML, Wang Y-X. Hemodynamic changes in apolipoprotein E-knockout mice. Am J Physiol Heart Circ Physiol 2000; 279: H2326–H2334.

Hartley CJ, Reddy AK, Madala S, Entman ML, Michael LH, Taffet GE. Noninvasive ultrasonic measurement of arterial wall motion in mice. Am J Physiol Heart Circ Physiol 2004;287:1426–1432.

Hope Simpson D, Chin CT, Burns PN. Pulse inversion Doppler: A new method for detecting nonlinear echoes from microbubble contrast agents. IEEE Trans Ultrason Ferroelect Freq Contr 1999;42:372–382.

Jensen JA. Estimation of blood velocities using ultrasound: A signal processing approach. New York: Cambridge University Press, 1996.

Kelly RC, Haywood C, Avolio AP, O'Rourke MF. Noninvasive determination of age-related changes in the human arterial pulse. Circulation 1989;80:1652–1659.

Latham RD, Westerhof N, Sipkema P, Rubal BJ, Reuderink P, Murgo JP. Regional wave travel and reflections along the human aorta: A study with six simultaneous micromanometric pressures. Circulation 1985;72:1257–1269.

Lehmann ED, Hopkins KD, Gosling RG. Aortic compliance measurements using Doppler ultrasound: *In vivo* biochemical correlates. Ultrasound Med Biol 1993;19:683–710.

Li JK. Dynamics of the vascular system. New Jersey: World Scientific, 2004.

Lukacs M, Yin J, Pang G, Garcia RC, Cherin E, Williams R, Mehi J, Foster FS. Performance and characterization of new micromachined high-frequency linear arrays. IEEE Trans Ultrason Ferroelect Freq Contr 2006;53:1719–1729.

Mitchell GF, Pfeffer MA, Finn PV, Pfeffer JM. Comparison of techniques for measuring pulse-wave velocity in the rat. J App Physiol 1997;82:203–210.

Nichols WW, O'Rourke MF. McDonald's blood flow in arteries, 3rd ed. London: Arnold, 1990.

O'Rourke MF, Staessen JA, Vlachopoulos C, Duprez D, Plante GE. Clinical application of arterial stiffness: Definitions and reference values. Am J Hypertens 2002;15:426–444.

Rabben SI, Stergiopulos N, Hellevik LR, Smiseth OA, Slordahl S, Urheim S, Angelsen B. An ultrasound-based method for determining pulse wave velocity in superficial arteries. J Biomech 2004;37:1615–1622.

Statistics Canada. Age-standardized mortality rates by selected causes, by sex: 2003. CANSIM, table 102–0552.

Sutton-Tyrrell K, Mackey RH, Holubkov R, Vaitkevicius PV, Spurgeon HA, Lakatta EG. Measurement variation of aortic pulse wave velocity in the elderly. Am J Hypertens 2001;14:463–468.

Zhang X, Greenleaf JF. Noninvasive generation and measurement of propagating waves in arterial walls. J Acoust Soc Am 2006;119: 1238–1243.